Received: 27 September 2020 | Revised: 26 November 2020 | Accepted: 16 February 2021

DOI: 10.1002/kjm2.12378

ORIGINAL ARTICLE

Kaohsiung Journal of Medical Sciences KJMS Open Access WILEY

Circular RNA circRNA_101996 promoted cervical cancer development by regulating miR-1236-3p/TRIM37 axis

Tie-Fang Song | Ai-Li Xu | Xiu-Hui Chen | Jia-Yin Gao | Fei Gao | Xian-Chao Kong

Department of Obstetrics and Gynecology, The Second Affiliated Hospital of Harbin Medical University, Harbin, China

Correspondence
Xian-Chao Kong, Department of Obstetrics and Gynecology, The Second Affiliated Hospital of Harbin Medical University, The Fifth Floor, Outpatient Building, No 246, Xuefu Road, Nangang District, Harbin, Heilongjiang, China.
Email: xianchaokongdgh@163.com

Funding information
Innovative Scientific Research Fund for Young and Middle-aged People of the Second Affiliated Hospital of Harbin Medical University, Grant/Award Number: KYCX2019-08

Abstract

Circular RNAs (circRNAs) appear to be significant modulators in various physiological processes. Recently, it is found that circRNA_101996 exerts important roles in various cancers. Our previous studies showed that circRNA_101996 promoted cervical cancer growth and metastasis by regulating miR-8075/TPX2. However, the potential regulatory role of circRNA_101996 in cervical cancer still needs further investigation. Our results in this study suggested that circRNA_101996 was over-expressed in cervical cancer patients. circRNA_101996 up-regulation remarkably assisted cell proliferation, cell cycle progression, and cell migration in cervical cancer, while circRNA_101996 knockdown exerted the inverse effects. The molecular investigations indicated that circRNA_101996 could increase the expression level of miR-1236-3p, tripartite motif-containing 37 (TRIM37), through binding to miR-1236-3p and reducing its expression. Moreover, in vivo results demonstrated that circRNA_101996 shRNA can function as a tumor suppressor through down-regulating TRIM37 in cervical cancer. In conclusion, our data indicated that circRNA_101996/miR-1236-3p/TRIM37 axis accelerated cervical cancer development, providing novel insights into cervical cancer diagnosis and treatment.

KEYWORDS
cell cycle, cell proliferation, cervical cancer, circRNA_101996, miR-1236-3p

1 | INTRODUCTION

Cervical cancer is considered one of the most common female malignant tumors globally. There are 450,000 new cases diagnosed with cervical cancer each year.[1–4] Despite the appearance and popularization of human papillomavirus (HPV) vaccine, the fatality rate of cervical cancer still ranks the second place in cancer-related deaths in women.[5] In particular, patients with advanced cervical cancer have extremely poor prognosis and low survival rate.[6] Thus, it is crucial to investigate the potential molecular mechanism in the development of cervical cancer, explore new biomarkers for diagnosis or treatment and figure out effective treatment strategies for cervical cancer.

Characterized as a covalently closed continuous loop, circRNAs have no 5′ to 3′ polarity and polyadenylation tails.[7] With the progress of high-throughput sequence, increasing circRNAs have been identified. However, their roles in carcinogenesis remain largely unclear. circRNA has a variety of regulatory roles, such as miRNA binding, protein interaction, and regulatory splicing.[8] MiRNAs are usually regulated by circRNA through the complementary binding sites.[9] It has been reported that miRNA can target genes within their

3′-untranslated region (3′-UTR).[10] Therefore, the sponge of circRNA to miRNA may alter gene expression, thereby forming a three-way functional axis of circRNA-miRNA-mRNA. According to our previous studies, circRNA_101996 could activate TPX2 expression by inhibiting mir-8075, which promoted the development of cervical cancer.[11] Nevertheless, whether there are other miRNAs that may be regulated by circRNA_101996 in cervical cancer deserves further research.

microRNAs (miRNAs) are epigenetic regulators that play different roles in the development of cancer. Recent evidences indicated that miR-1236-3p expression was frequently reduced in gastric cancer tissues, and closely associated with poor prognosis of gastric cancer patients, which may be a new diagnostic and prognostic biomarker.[12–13] Besides, the suppressive roles of miR-1236-3p were demonstrated in lung adenocarcinoma and ovarian carcinoma.[14–15] However, the role of miR-1236-3p in cervical cancer is still unknown.

As evolutionarily conserved proteins, tripartite motif-containing (TRIM) family proteins, contain some domains, such as ring finger domain, B-box domains, and coiled coil domain, which are found to be related to multiple cellular processes.[16–17] TRIM37 (tripartite motif-containing 37) serves as an E3 ubiquitin ligase and is related to the K63 polyubiquitination of TRAF2, which eventually activates NF-κB pathway.[18] TRIM37 expression at mRNA and protein levels was identified in non-small-cell lung cancer (NSCLC), which was closely related to the morbidity and prognosis of NSCLC patients.[19] Inhibition of TRIM37- by LSD1, a histone demethylase, led to down-regulated level of some cell adhesion-associated genes and subsequently breast cancer metastasis.[20] In addition, the function of TRIM37 in promoting tumor growth and metastasis has been demonstrated in many other cancers, such as liver cancer, gastric carcinoma, and colon cancer.[21–23] However, the role of circRNA_101996 in cervical cancer needs to be elucidated.

In this study, we determined the circRNA_101996 expression in cervical cancer tissues and explored the effects of circRNA_101996 on cervical cancer cell proliferation, cell cycle, and cell migration. StarBase analysis was used to predict circRNA_101996's potential target miRNAs. Luciferase report assay was then used to confirm the targeting relationship. Based on TargetScan analysis, we found that miR-1236-3p might target the 3′-UTR of TRIM37. Therefore, we speculated that circRNA_101996 might promote cervical cancer development by regulating TRIM37 expression by sponging miR-1236-3p. Biological functions and regulatory ways of circRNA_101996/miR-1236-3p/TRIM37 axis in cervical cancer development were systematically explored, which may help to exploit new diagnostic and therapeutic candidates for cervical cancer.

2 | MATERIALS AND METHODS

2.1 | Tissue samples of patients

Paired cervical cancer tissues (tumor) and normal adjacent tissues (normal) were collected at The Second Affiliated Hospital of Harbin Medical University. No cervical cancer patients got any chemotherapy or radiotherapy before section. The collection and experiments have received the permission of the Ethics Committee of The Second Affiliated Hospital of Harbin Medical University (Approval no. KY2019-060). Informed consents were signed and gathered from patients. Pathological diagnostics were completed by three pathologists, respectively. For clinical information of cervical cancer patients, see Table 1.

2.2 | RNA extraction and quantitative real-time PCR

TRIzol reagent (Thermo Fisher Scientific, Rockford, IL) was used to extract total RNAs from cervical cancer cells and tissues. Nucleus and cytoplasm were separated using an extraction Kit (inventbiotech, Beijing, China). A PrimeScript RT Reagent Kit (Takara, Shiga, Japan) was used to synthesize cDNA from total RNA. Quantitative real-time PCR (qRT-PCR) assays for genes were conducted by using SYBR Premix Ex Taq (Takara). SYBR PrimeScript miRNA RT-PCR Kit (Takara) was applicated to quantity miRNA expressions. To normalize circRNA_101996 and TRIM37 mRNA levels, phosphoglyceraldehyde dehydrogenase (GAPDH) was selected as internal control. U6 snRNA was used to normalize miRNA expressions. The corresponding primer sequences were listed in Table S1.

2.3 | Overall survival analysis

After qRT-PCR analysis, the mean circRNA_101996 level was calculated and used as a criterion to estimate the expression of circRNA_101996. If circRNA_101996 level exceed the mean value, high expression level was identified. When the circRNA_101996 level was under the average value, low expression level was classified. According to patients' follow-up data, overall survival curves were analyzed by the Kaplan–Meier method.

TABLE 1 Relationship between circRNA_101996 expression and clinicopathological factors

	circRNA_101996 expression		
Characteristics	**Low (n = 30)**	**High (n = 30)**	***p* value**
Age (years)			0.196
≥50	17	12	
<50	13	18	
Lymph node metastasis			0.038*
Yes	10	18	
No	20	12	
Tumor size (cm)			0.020*
<4	18	9	
≥4	12	21	
Clinical stage			0.004*
I/II	19	8	
III/IV	11	22	

*$p < 0.05$.

2.4 | Cell culture

Human cervical epithelial cells (HCerEpiC) and several cervical cancer cell lines (C33A, Hela, SiHa, and CaSki) were purchased from American type culture collection (ATCC) cell lines (Manassas, VA) and used in the present study. CaSki cells were cultured in RPMI-1640 Medium.

Eagle's minimum essential medium was used to culture HCerEpiC, Hela and SiHa cells, and Dulbecco's modified eagle medium was used for culture C33A cells. Ten percent of FBS (Thermo Fisher Scientific) was added into cell medium. Cells were cultured in a humidified atmosphere with 5% CO_2 at 37°C.

2.5 | Cell transfection

SiHa or CaSki cells were transfected with shRNA for circRNA_101996 (sh-circ#1, sh-circ#2), circRNA_101996 expressing plasmid (OE-circRNA), miR-1236-3p-mimics (miR-1236-3p), miR-1236-3p inhibitors (miR-1236-3p inh), TRIM37 expressing plasmid (TRIM37) or the relevant controls (sh-NC, NC, miR-NC, inh NC, shNC, or Con) using lipofectamine 2000 (Thermo Fisher Scientific). Two shRNAs for circRNA_101996 were tested, and the more efficient one (sh-circ #1, 5′-GCCAAGGGG CCTTTACAACAA-3′) was used for following experiments.

2.6 | Cell growth assay

After transfected with sh-NC, sh-circ, NC, OE-circRNA, inh NC + sh-NC, inh NC + sh-circRNA, sh-circRNA+miR-1236-3p inh, miR-NC + Con, miR-1236-3p + Con, or miR-1236-3p + TRIM37, the proliferation curves of SiHa or CaSki cells were, respectively, determined. First, cells were seeded in 96-well plates (6×10^3 cells/per well). Then, a cell counting kit-8 (CCK-8, Dojindo, Tokyo, Japan) was selected to determine the number of viable cells after cultured for 0, 24, 48, 72, 96 h. A microplate spectrometer (Thermo Fisher Scientific) was used to determine the absorbance (OD = 450 nm).

To perform colony formation assay, SiHa or CaSki cells (1×10^3) were primarily plated onto top agar (1.5 ml). After that, the mixture was added onto base agar. Crystal Violet was used to stain colonies after 3 weeks. The colonies could be counted by dissection microscope (Nikon, Tokyo, Japan).

Thymidine analog 5-ethynyl-2′-deoxyuridine (EDU) incorporated into DNA during DNA replication was used to monitor cells. Cells were fixed and incubated with EDU (50 μM, 3 h). Then, 4, 6-diamidine-2-phenyl indole (DAPI) (1 μg/ml, 10 min) was used to stain cells. A fluorescence microscopy (Nikon) was used to count the EDU positive cells.

2.7 | Cell cycle assay

For cell cycle assay, SiHa or CaSki cells were harvested 48 h post-transfection. Cells were primarily fixed by ethanol (70%). After that, cells were treated by RNase A (100 μg/ml, Takara) as well as propidium iodide (PI, 50 μg/ml, Sigma-Aldrich, St. Louis, MO). To analyze DNA content, FACSCalibur system (BD Biosciences, San Jose, CA) and ModFit_LT software were applied.

2.8 | Cell migration assay

For wound scratch assay, linear scratch wounds were conducted on the cell monolayer. After 24 h, an inverted microscope (Nikon) was used to take photos of cell migration. Then, the distances of the scrape were determined using an image J software (http://rsb.info.nih.gov/ij/).

For transwell assay, SiHa or CaSki cells (1×10^5) were cultured in the top chamber of a Matrigel (BD Biosciences) pre-coated insert (Corning Costar Co., Cambridge, MA). In the top chamber, cells were cultured using serum-free medium. Cell culture medium with FBS (10%) was added into the lower chamber. Twelve hours later, the invaded cells fixed. And cells underside of the membrane were then stained, imaged, and counted.

2.9 | Western blotting

Protein was extracted by radio-immunoprecipitation issay (RIPA) lysis buffer (Sigma-Aldrich) and quantified by a bicinchoninic acid (BCA) protein assay kit (Thermo Fisher Scientific). Antibodies including E-cadherin, N-cadherin, TRIM37, GAPDH, and corresponding secondary antibodies were used in this study. After Vertical electrophoresis by SDS-PAGE, proteins were transferred onto PVDF membrane. The polyvinylidene fluoride (PVDF) membrane was later incubated with the primary antibodies (overnight at 4°C) after blocking with 5% skim milk. After that, an HRP (horseradish peroxidase) was used to conjugate with anti-mouse IgG (Thermo Fisher Scientific). To normalize target protein levels, GAPDH was used. Antibody information was showed in Table S2.

2.10 | In situ hybridization

In situ hybridization (ISH) assay was performed to detect the fluorescence of circRNA_101996 and miR-1236-3p using An ISH kit (Thermo Fisher Scientific) as previously reported.[24] Cells were fixed in paraformaldehyde, blocked in pre-hybridization buffer, incubated with a circRNA_101996 probe conjugated by Cy5 or a miR-1236-3p probe conjugated by fluorescein isothiocyanate (FITC, Exiqon, Vedbaek, Denmark) in hybridization buffer, and finally stained by DAPI (Sigma-Aldrich). Fluorescence images were acquired by a Nikon confocal microscope (Nikon, Tokyo, Japan). Immunofluorescence experiments were independently performed three times.

2.11 | Plasmids

The sequence of circRNA_101996 was amplified using a human genomic DNA and inserted into the PCI or p-MIR-reporter plasmid (Promega, Madison, WI). The mutant luciferase plasmid (binding site: GGAAGAG substituted by CCUUCUC) was also used as a control.

According to the methods above, the p-MIR-reporter plasmid containing the 3′-UTR of TRIM37 was obtained. In addition, the corresponding mutant luciferase plasmid (binding site: GGGAAGAG substituted by CCCUUCUC) was constructed as a negative control. Primers sequences were listed in Table S3.

2.12 | Luciferase reporter assay

Luciferase reporter assays were conducted as previously reported.[25] When cell confluence reached 70%–80%, β-galactosidase expression vector (Promega), firefly luciferase reporter plasmid, and miR-1236-3p or miR-NC were co-transfected into SiHa or CaSki cells. After 24 h, luciferase activities were determined by means of a Luciferase Reporter Assay System (Promega).

2.13 | RNA binding protein immunoprecipitation assay

RNA binding protein immunoprecipitation assay was performed as previously reported.[26] Ago2 antibodies or IgG were used to incubate the cell lysates of SiHa or CaSki cells. RNA was extracted from the pull down complexes, and circRNA_101996 and miR-1236-3p levels were then determined using qRT-PCR.

2.14 | Cervical cancer xenograft mouse model

Animal experiments were operated according to the Guidelines for the Care and Use of Laboratory Animals published by the National Institutes of Health[27] and approved by the Ethics Committee XXX University (Approval no. XXX). To establish a cervical cancer xenograft mouse model, thymic BALB/c nude mice (16–18 g) were used. First, recombinant lentivirus was used to construct SiHa cells stably expressing circRNA_101996 shRNA (sh-circ) or the corresponding control cells (sh-NC). After that, mice (six mice/group) were subcutaneously injected with these cells (1×10^6) at the right flanks. 3, 6, 9, 12, 15, 18, and 21 days later, tumor volume of each group was calculated using the formula of $V = 1/2LW^2$, where W and L, respectively, represent the long and wide tumor diameters. Twenty-one days post-implantation, the tumors were acquired from mice, weighted and imaged. In addition, hematoxylin and eosin (H&E) staining and immunohistochemistry (IHC) analysis of TRIM37, Ki-67, E-cadherin, and N-cadherin in the tumor tissues were conducted, respectively. Based on the Pearson's correlation analysis, correlations among circRNA_101996, miR-1236-3p, and TRIM37 mRNA levels in xenograft tumors were analyzed.

2.15 | Statistical analysis

Results were presented as the mean ± SEM. Student's t-test was used to analyze the statistical differences between two groups, and one-way analysis of variance was used for multiple groups. Assays were independently conducted for at least three times. The correlations between circRNA_101996 and miR-1236-3p, miR-1236-3p and TRIM37 mRNA, circRNA_101996 and TRIM37 mRNA were, respectively, determined by Pearson correlation analysis. $p < 0.05$ was classified as significant. */#, $p < 0.05$; **/##, $p < 0.01$.

3 | RESULTS

3.1 | circRNA_101996/miR-1236-3p/TRIM37 axis was associated with cervical cancer

To study the interrelation between circRNA_101996/miR-1236-3p/TRIM37 and cervical cancer development, we determined their levels in cervical cancer tissues (tumor, $n = 60$) and adjacent normal tissues (normal, $n = 60$). The results suggested that the level of circRNA_101996 was significantly over-expressed in cervical cancer samples compared with normal samples (Figure 1A). We found that circRNA_101996 expression levels were correlated with clinical pathological parameters (Table 1). As shown in Figure 1A, the circRNA_101996 expression level in patients at stage III/IV was higher than that of patients at stage II, which was higher than that of patients at stage I. The patients groups with positive lymph node metastasis (LNM) or larger tumor sizes (≥4 cm) had higher circRNA_101996 levels compared to the groups with negative LNM or smaller tumor sizes (<4 cm). Then, the relationships between survival of cervical cancer patients and the circRNA_101996 level were analyzed by Kaplan–Meier method. As shown in Figure S1A, cervical cancer patients with high circRNA_101996 expression had a relatively lower survival rate. In addition, circRNA_101996 expressions in four cervical cancer cell lines (C33A, Hela, SiHa, and CaSki) were higher than that in human cervical epithelial cells (HCerEpiC, Figure S1B). Among the cervical cancer cells, SiHa and CaSki had higher circRNA_101996 expressions, thus these two cell lines were selected to investigate the role of circRNA_101996 in cervical cancer. RNase R is a ribonuclease that can degrade linear RNA, but is not efficient for circular RNA. As shown in Figure S1C, RNase R could degrade the linear transcript of GAPDH. However, RNase R treatment was not applicable for circRNA_101996. The above data revealed that circRNA_101996 is up-regulated in cervical cancer tissues and cells.

In addition, we also determined miR-1236-3p levels in patients. The results suggested that miR-1236-3p level was markedly down-regulated in cervical cancer tissues (Figure 1B). Through Pearson's correlation analysis, a negative relationship between miR-1236-3p and circRNA_101996 in tissues of cervical cancer patients was demonstrated (Figure 1C). Furthermore, we determined TRIM37 mRNA levels in patient tissues by qRT-PCR. The results demonstrated that TRIM37 mRNA levels were significantly increased in cervical cancer patients (Figure 1D). Based on the Pearson's correlation analysis, a negative relationship between miR-1236-3p and TRIM37 mRNA levels, and a positive relationship between circRNA_101996 and TRIM37 mRNA levels were found in cervical cancer patients

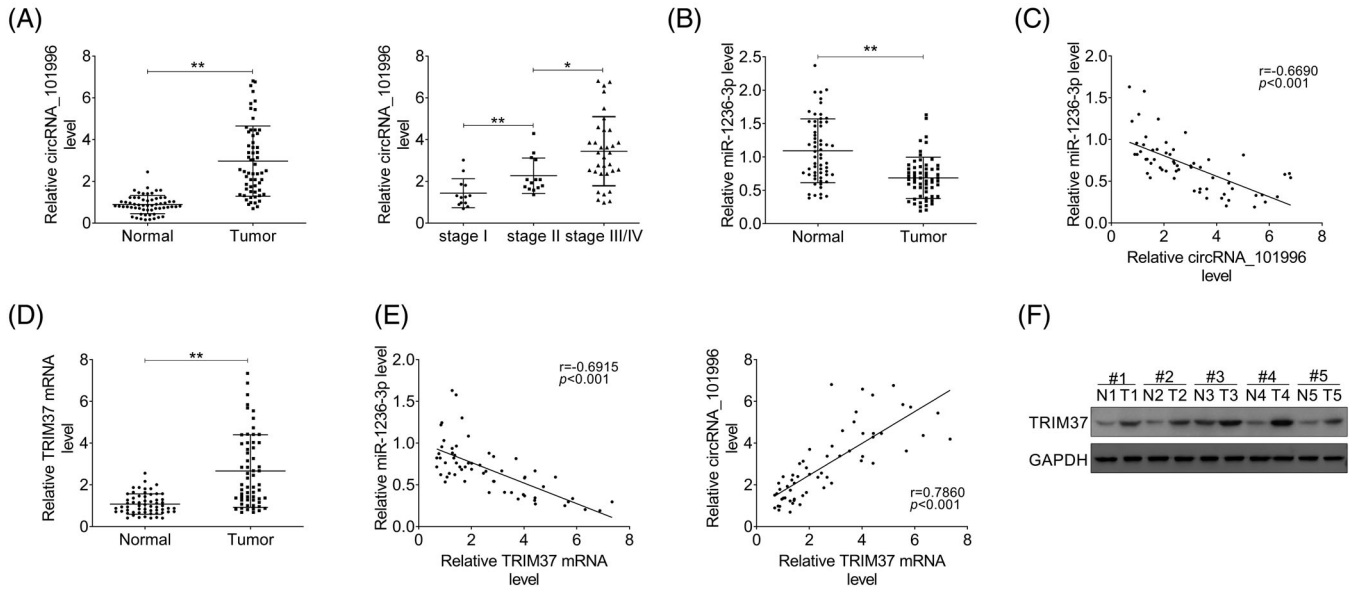

FIGURE 1 circRNA_101996/miR-1236-3p/TRIM37 axis was associated with cervical cancer. (A) Relative circRNA_101996 expression levels in cervical cancer tissues (tumor, $n = 60$) and normal adjacent tissues (normal, $n = 60$), as determined using qRT-PCR. Relative circRNA_101996 expression levels in cervical cancer tissues (tumor, $n = 60$), stratified by tumor stages (I, II, or III/IV), lymph node metastasis (LNM, no, or yes), and tumor sizes (<4 cm or ≥4 cm). (B) Relative miR-1236-3p levels in cervical cancer tissues (tumor, $n = 60$) and normal adjacent tissues (normal, $n = 60$), as determined using qRT-PCR. (C) Pearson's correlation analysis of the relative expressions between miR-1236-3p and circRNA_101996. (D) TRIM37 mRNA levels in cervical cancer tissues (tumor, $n = 60$) and normal adjacent tissues (normal, $n = 60$), as determined using qRT-PCR. (E) Pearson's correlation analysis of the relative expressions between miR-1236-3p and TRIM37 mRNA, circRNA_101996 and TRIM37 mRNA in cervical cancer patients. (F) TRIM37 protein levels in cervical cancer tissues (tumor, $n = 5$) and normal adjacent tissues (normal, $n = 5$), as determined using western blotting (mean ± SEM, */#$p < 0.05$, **/##$p < 0.01$)

(Figure 1E). Western blot data also revealed that TRIM37 protein level was markedly up-regulated in tissues of cervical cancer patients (Figure 1F). These data revealed that the axis of circRNA_101996/miR-1236-3p/TRIM37 was associated with cervical cancer, which may exert an important function in cervical cancer.

3.2 | CircRNA_101996 affected cell proliferation, cell cycle progression, and cell migration in cervical cancer

qRT-PCR and ISH were performed to study the expression and distribution of linear and circular RNA. As shown in Figures S2A and S2B, circular RNA was expressed in both cytoplasm and nucleus, but was primarily expressed in cytoplasm. The expression of circRNA_101996 was significantly reduced upon sh-circ#1 and sh-circ#2 transfection compared with sh-NC transfected cells, and OE-circRNA transfection led to up-regulation of circRNA_101996 (Figure S2C). Cell proliferation was suppressed in SiHa or CaSki cells transfected with circRNA_101996 shRNA, and was promoted in cells transfected with OE-circRNA (Figure S2D). Colony formation assay showed that down-regulation of circRNA_101996 markedly inhibited the colony formation, and circRNA_101996 over-expression increased the colony numbers (Figure S2E). In addition, cell numbers of SiHa or CaSki cells incorporating EDU were markedly decreased in the sh-circ-treated group and up-regulated in the OE-circRNA-treated group contrast compared with the control cells (Figure S2F). Furthermore, down-regulation of circRNA_101996 in SiHa or CaSki cells led to an up-regulated G1-phase cell population and a decreased S-phase cell population. In the contrast, circRNA_101996 over-expression in SiHa or CaSki cells resulted in a down-regulated G1-phase cell population and an increased S-phase cell population (Figure S2G).

Moreover, the effects of circRNA_101996 on cell migration were studied by means of wound scratch healing, transwell and western blot assays. The results indicated that the mobility of SiHa or CaSki cells was significantly inhibited after sh-circ treatment and was promoted after OE-circRNA treatment (Figure S3A). In addition, the number of migrated SiHa or CaSki cells transfected with sh-circ was significantly reduced, and markedly increased in cells transfected with OE-circRNA (Figure S3B). In addition, the protein level of E-cadherin was significantly up-regulated upon sh-circ treatment and was inhibited after OE-circRNA treatment compared with the control cells. While, the protein level of N-cadherin was markedly suppressed upon sh-circ treatment and was up-regulated after OE-circRNA treatment (Figure S3C). Furthermore, wound scratch healing and transwell assays were performed using C33A, HeLa, Siha, CaSki cells. The results showed that SiHa or CaSki cells with a higher circRNA_101996 levels had higher metastatic properties (Figure S4). Together, these

data e suggested that down-regulation of circRNA_101996 could suppress the cell proliferation, cycle progression and migration in cervical cancer, while over-expression of circRNA_101996 had an opposite effect on cervical cancer cells.

3.3 | CircRNA_101996 directly sponged miR-1236-3p and negatively adjusted its expression

CircRNA_101996 was demonstrated to affect some cell biological functions, such as cell proliferation, cell cycle progression and cell migration. However, the molecular mechanisms remain unknown. Thus, we analyze the potential miRNA that could be targeted by circRNA_101996. By using starBase (http://starbase.sysu.edu.cn/starbase2/), we predicted that circRNA_101996 may bind to miR-1236-3p. Binding affinity of circRNA_101996 with miR-1236-3p was predicted (Hybridization $\Delta G = -24.3$ kcal/mol). The ISH results in Figure 2A showed that Cy5 fluorescence of circRNA_101996 was mostly overlapped with FITC fluorescence of miR-1236-3p, and they were mainly co-localized in cytoplasm. As shown in Figure 2B, the potential base pairing between miR-1236-3p and circRNA_101996 were predicted. Up-regulation of miR-1236-3p suppressed the luciferase activity of the circRNA_101996 reporter plasmids. However, after the binding sites were mutated, miR-1236-3p up-regulation could not cause remarkable changes of luciferase activities (Figure 2C). Furthermore, both circRNA_101996 and miR-1236-3p were significantly enriched by Ago2 antibody (Figure 2D). Because Ago2 is a vital member of RISC protein complex mediated by miRNA, this result ulteriorly suggested the bond between miR-1236-3p and circRNA_101996. Altogether, these results revealed that circRNA_101996 negatively regulated miR-1236-3p in cervical cancer cells.

3.4 | miR-1236-3p negatively adjusted TRIM37 by binding to its 3′-UTR

In cervical cancer cells, circRNA_101996 could target miR-1236-3p. However, the role miR-1236-3p in cervical cancer remains to be elucidated. Then, we predicted the target gene of miR-1236-3p by means of TargetScan, and TRIM37 stood out. The potential binding sites between miR-1236-3p and TRIM37 were depicted in Figure 3A. As shown in Figure 3B, over-expression of miR-1236-3p suppressed the luciferase activity of the TRIM37 3′-UTR reporter plasmids. However, after we mutated miR-1236-3p's binding sites, its over-expression did not lead to remarkable changes of luciferase activities. As shown in Figure 3C, the miR-1236-3p level was significantly up-regulated after miR-1236-3p transfection compared to miR-NC transfected cells. Accordingly, miR-1236-3p inhibitors (miR-1236-3p inh) markedly reduced miR-1236-3p levels. qRT-PCR (Figure 3C) and western blot (Figure 3D) results demonstrated that TRIM37 mRNA and protein expression levels were markedly reduced after miR-1236-3p transfection, and miR-1236-3p inhibitors led to opposite effects. These findings indicated that miR-1236-3p may negatively regulate TRIM37 by binding to its 3′-UTR in cervical cancer.

3.5 | CircRNA_101996 affected cervical cancer cell proliferation, cycle progression, and migration by suppressing miR-1236-3p

So far, our results revealed that circRNA_101996 can affect cell proliferation, cell cycle progression, and cell migration in cervical cancer. And circRNA_101996 could sponge miR-1236-3p. Then, we studied the effect of circRNA_101996/miR-1236-3p axis on cervical cancer cells. As shown in Figure 4A, cell proliferation was suppressed after knocking down circRNA_101996, which could be abolished b inhibition of miR-1236-3p. Colony formation assay indicated that down-regulation of circRNA_101996 markedly reduced the numbers of colony formation, and the colony formation numbers could be restored by sh-circRNA+miR-1236-3p inh treatment (Figure 4B). The cell number of SiHa or CaSki cells incorporating EDU was decreased in the sh-circ-treated group, and treatment of sh-circRNA+miR-1236-3p inh rescued the numbers of EDU-incorporated cells, compared to the inh NC + sh-NC control cells (Figure 4C). In addition, sh-circRNA would significantly increase G1-phase cell population and decrease S-phase cell population in SiHa or CaSki cells (Figure 4D). However, circRNA_101996 inhibition caused-cell cycle delay could be rescued by knocking down of miR-1236-3p. The mobility of SiHa or CaSki cells was markedly suppressed in the condition of circRNA_101996 suppression, which was weakened upon the treatment of sh-circRNA +miR-1236-3p inh (Figure 5A). As shown in Figure 5B, the migrated cell number upon sh-circRNA treatment was significantly reduced, compared to those treated with inh NC + si-NC. Whereas, simultaneously knocking down of circRNA_101996 and miR-1236-3p greatly up-regulated the migrated the cell number. In addition, western blot results suggested that down-regulation of circRNA_101996 reduced the protein expressions of E-cadherin and elevated the protein levels of N-cadherin. Moreover, synchronous suppression of miR-1236-3p and circRNA_101996 eliminated sh-circRNA-caused expression changes of these two metastasis related proteins, E-cadherin and N-cadherin (Figure 5C). These results indicated that circRNA_101996 down-regulation inhibited the cell proliferation, cell cycle progression, and cell migration in cervical cancer, by negatively regulating miR-1236-3p expression.

3.6 | miR-1236-3p affected cervical cancer cell proliferation, cycle progression, and migration by inhibiting TRIM37

The above results revealed that circRNA_101996 can affect cell proliferation, cell cycle progression, and cell migration in cervical cancer by regulating miR-1236-3p. Because miR-1236-3p could target TRIM37. Then, we studied the effect of miR-1236-3p/TRIM37 axis on cervical cancer cells. As shown in Figure 6A, cell proliferation was

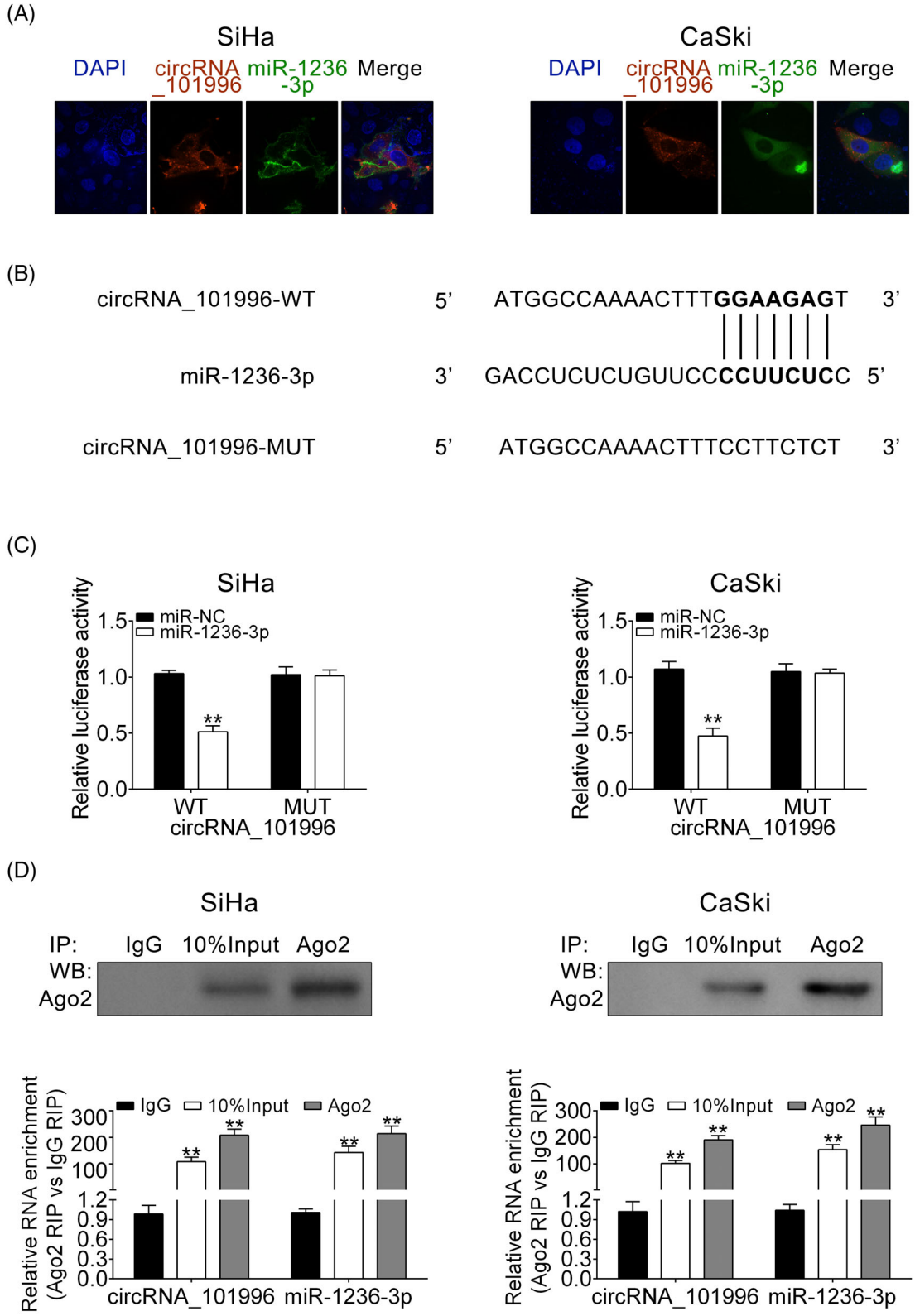

FIGURE 2 circRNA_101996 could directly bind to miR-1236-3p and negatively regulate its expression. (A) Co-location detection of circRNA_101996 and miR-1236-3p in SiHa or CaSki cells using ISH. (B) StarBase prediction identified seeds match for circRNA_101996 in the mature sequence of miR-1236-3p. The predicted seed-recognition site in the miR-1236-3p sequence and the corresponding circRNA_101996 sequence is marked in bold. (C) Relative luciferase activity of the circRNA_101996 reporter plasmid in SiHa or CaSki cells upon miR-1236-3p or the miR-NC transfection. The mutant circRNA_101996 reporter was used as a negative control. (D) SiHa or CaSki cells were harvested and incubated with Ago2 antibodies to perform RNA binding protein immunoprecipitation (RIP) assay. circRNA_101996 or miR-1236-3p levels were tested by qRT-PCR and compared to the groups of IgG and input (mean ± SEM, $^{**}p < 0.01$)

suppressed after overexpressing miR-1236-3p, which could be abolished when up-regulating miR-1236-3p and TRIM37 together. Colony formation assay indicated that miR-1236-3p up-regulation markedly reduced the number of colony formation, and the colony formation number could be restored by miR-1236-3p + TRIM37 treatment (Figure 6B). Cell numbers of SiHa or CaSki cells incorporating EDU were decreased in the miR-1236-3p + Con group, and treatment of miR-1236-3p + TRIM37 rescued the numbers of EDU-incorporated cells, compared to the miR-NC + Con cells (Figure 6C). In addition, miR-1236-3p would result in a significant up-regulated G1-phase cell population and a decreased S-phase cell population in SiHa or CaSki cells (Figure 6D). However, miR-1236-3p caused-cell cycle delay could be rescued by overexpressing miR-1236-3p and TRIM37 together. The mobility of SiHa or CaSki cells was markedly suppressed by miR-1236-3p expression, which was weakened upon the treatment of miR-1236-3p + TRIM37 (Figure 7A). As shown in Figure 7B, migrated cell numbers upon miR-1236-3p treatment were significantly reduced, compared to those upon miR-NC + Con treatment. Whereas, up-regulating miR-1236-3p and TRIM37 together greatly up-regulated the migrated cell numbers. In addition, western blot results suggested that up-regulation of miR-1236-3p reduced the protein expressions of E-cadherin and elevated the protein levels of N-cadherin. Moreover, synchronous overexpression of miR-1236-3p and TRIM37 eliminated miR-1236-3p-caused expression changes of these two metastasis correlative proteins, E-cadherin and N-cadherin (Figure 7C). These results indicated miR-1236-3p inhibited the cell proliferation, cell cycle progression, and cell migration in cervical cancer, by negatively regulating TRIM37 expression.

3.7 | CircRNA_101996 down-regulation inhibited tumor growth in a mouse xenograft model

Since circRNA_101996 inhibition down-regulated the cell proliferation, cell cycle progression, and cell migration in vitro, the role of circRNA_101996 was whereafter studied in vivo. To construct a xenograft tumor mouse model, SiHa cells stably expressing shRNA interfering circRNA_101996 was established. As shown in Figure 8A, at 21 days post-implantation, significant down-regulated circRNA_101996 level and increased miR-1236-3p level were found in xenograft tumors from the sh-circ group compared to those in sh-NC groups. The corresponding tumors were excised and showed in Figure 8B. The tumor sizes of sh-circ group mice were significantly smaller than those in sh-NC group, and the tumor weight of sh-circ group mice was reduced (Figure 8C). The degree of infiltration of tumor cells was significantly reduced in xenograft tumors of the sh-circ group after histopathological analysis (Figure 8D). Furthermore, down-regulation of circRNA_101996 decreased the expression of TRIM37 and Ki-67 positive cell number, up-regulated E-cadherin level as well as decreased N-cadherin expression in xenograft tumors (Figure 8E). According to the Pearson's correlation analysis, a negative relationship

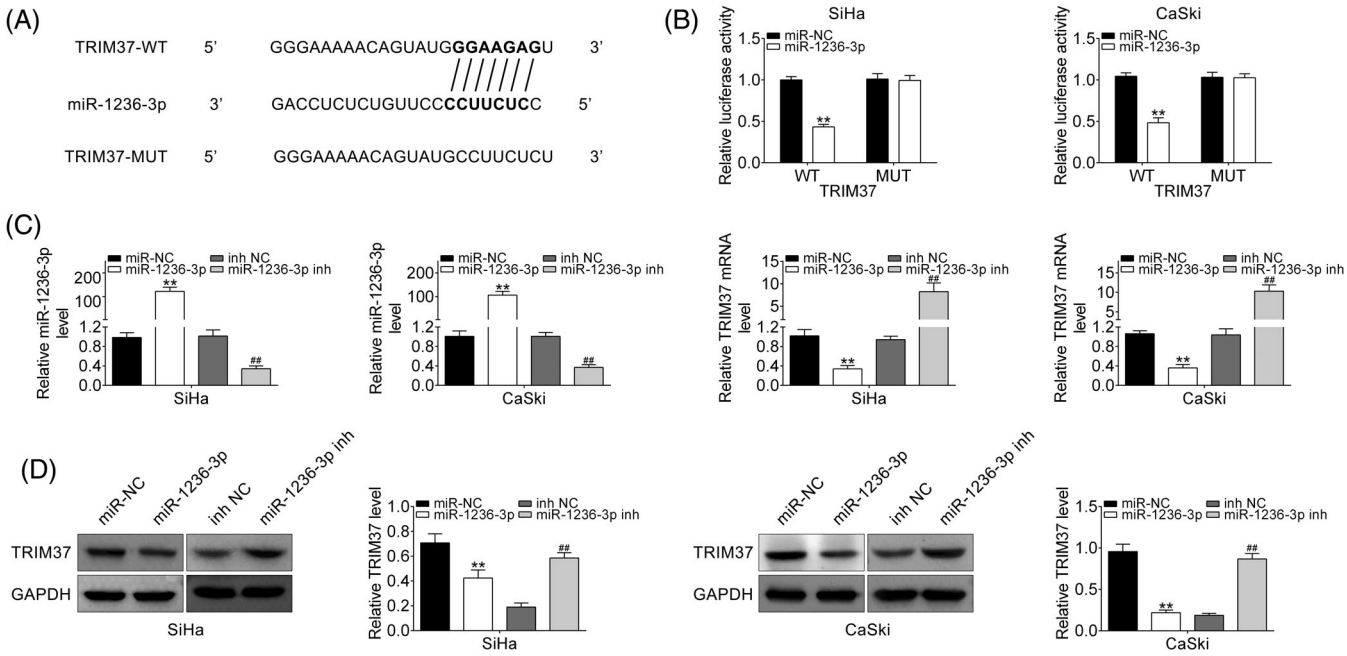

FIGURE 3 miR-1236-3p negatively regulates TRIM37 through targeting its 3′-UTR. (A) TargetScan prediction software identified seeds match for miR-1236-3p in the 3′-UTR of TRIM37; the predicted seed-recognition sites in the TRIM37 mRNA sequence and the corresponding miR-1236-3p sequence are marked in bold. (B) Relative luciferase activity of the TRIM37 3′-UTR reporter plasmid was measured in SiHa or CaSki cells after expressing miR-1236-3p or miR-NC. The mutant TRIM37 3′-UTR reporter was used as a negative control. (C) Relative miR-1236-3p (left) and TRIM37 mRNA (right) expression levels in SiHa or CaSki cells after transfected with miR-1236-3p, miR-1236-3p inh, miR-NC, or inh NC, as determined using qRT-PCR. (D) TRIM37 protein levels in SiHa or CaSki cells after transfected with miR-1236-3p, miR-1236-3p inh, miR-NC, or inh NC, as determined using western blotting. Bands and images were quantified by image J and shown as histogram (mean ± SEM, $^{**}p < 0.01$)

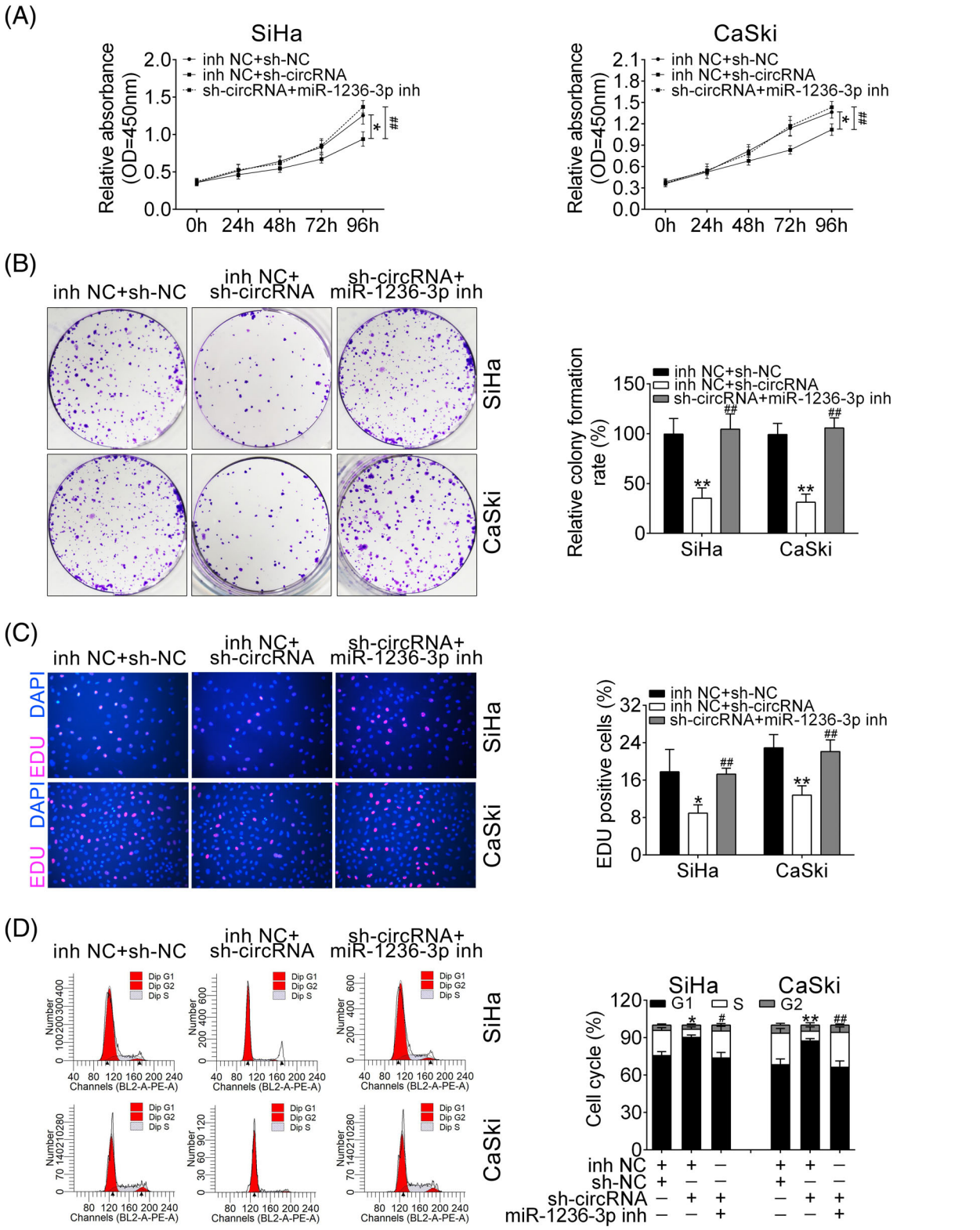

FIGURE 4 circRNA_101996/miR-1236-3p affected the proliferation and cycle progression of cervical cancer cells. (A) Growth curves of SiHa or CaSki cells after transfection with inh NC + sh-circRNA, sh-circRNA+miR-1236-3p inh, or the corresponding control (inh NC + sh-NC). Measurements of the cell growth rate were obtained using a CCK-8 kit. (B) Colony formation analysis of SiHa or CaSki cells expressing inh NC + sh-circRNA, sh-circRNA+miR-1236-3p inh, or inh NC + sh-NC. Colony numbers were quantified. (C) Representative profiles of EDU cell growth in SiHa or CaSki cells after transfection with inh NC + sh-circRNA, sh-circRNA+miR-1236-3p inh, or inh NC + sh-NC. EDU positive cell numbers were quantified. (D) Cell cycle analysis of SiHa or CaSki cells after transfection with inh NC + sh-circRNA, sh-circRNA+miR-1236-3p inh, or inh NC + sh-NC. Cell percentage in G1, S, and G2 phages were quantified (mean ± SEM, */#$p < 0.05$, **/##$p < 0.01$)

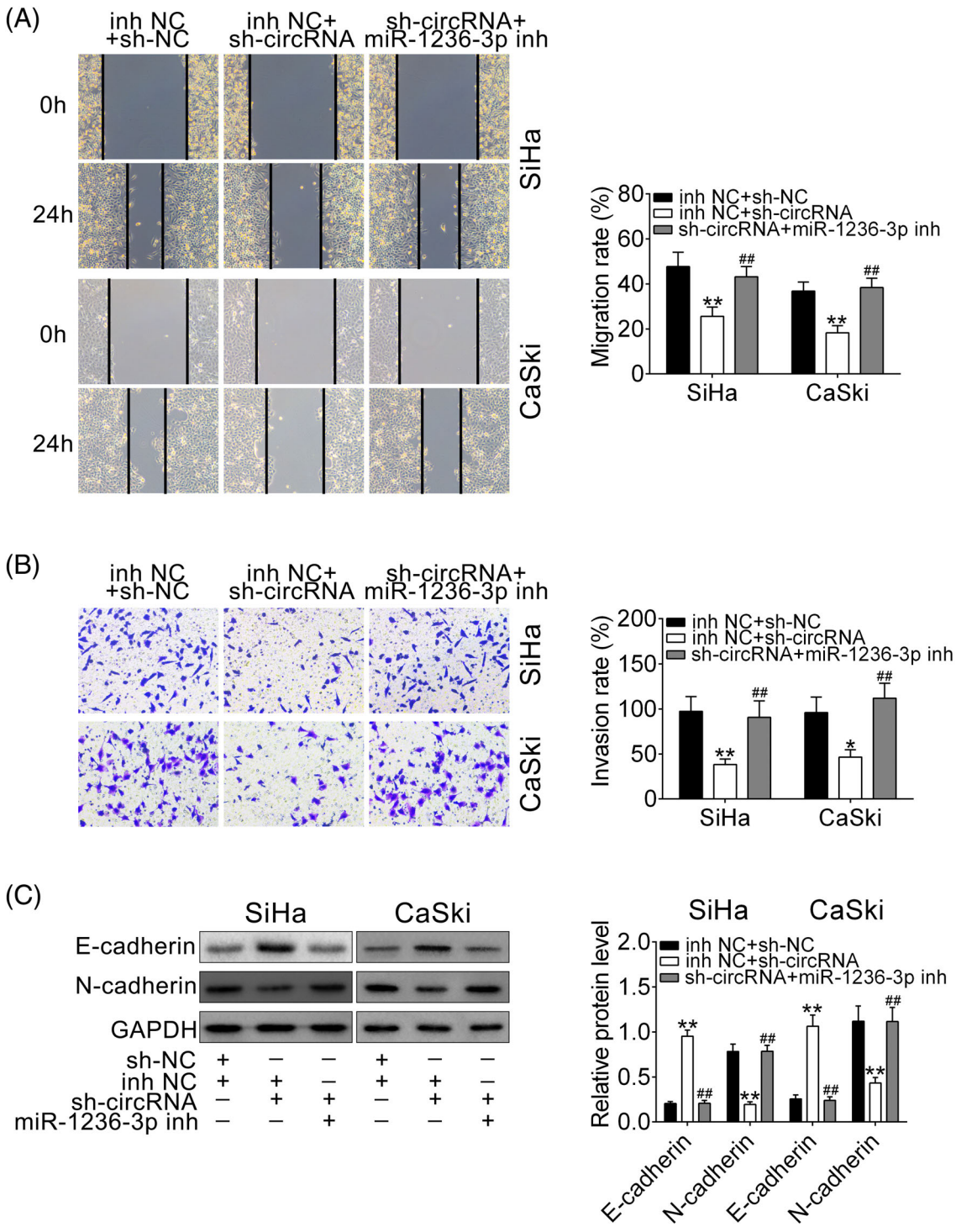

FIGURE 5 circRNA_101996/miR-1236-3p affected the migration of cervical cancer cells. (A) Wound scratch healing assay of SiHa or CaSki cells after transfection with inh NC + sh-circRNA, sh-circRNA+miR-1236-3p inh, or inh NC + sh-NC. Quantification of the wound-healing assay was shown as histograms. (B) Migration assay of SiHa or CaSki cells inh NC + sh-circRNA, sh-circRNA+miR-1236-3p inh, or inh NC + sh-NC. The migrated cells were quantified and shown as histograms. (C) Protein expression levels of E-cadherin and N-cadherin in SiHa or CaSki cells inh NC + sh-circRNA, sh-circRNA+miR-1236-3p inh, or inh NC + sh-NC, as determined using western blotting. Bands and images were determined by image J and shown in histogram (mean ± SEM, $^{*}p < 0.05$, $^{**}/\#\#p < 0.01$)

between circRNA_101996 and miR-1236-3p levels, a negative relationship between miR-1236-3p and TRIM37 mRNA levels, and a positive relationship between circRNA_101996 and TRIM37 mRNA levels were observed in xenograft tumors (Figure 8F). Together, these findings revealed that down-regulation of circRNA_101996 could up-regulate miR-1236-3p level, suppress TRIM37's protein expression, decrease tumor growth and thus inhibit the cervical cancer development in vivo.

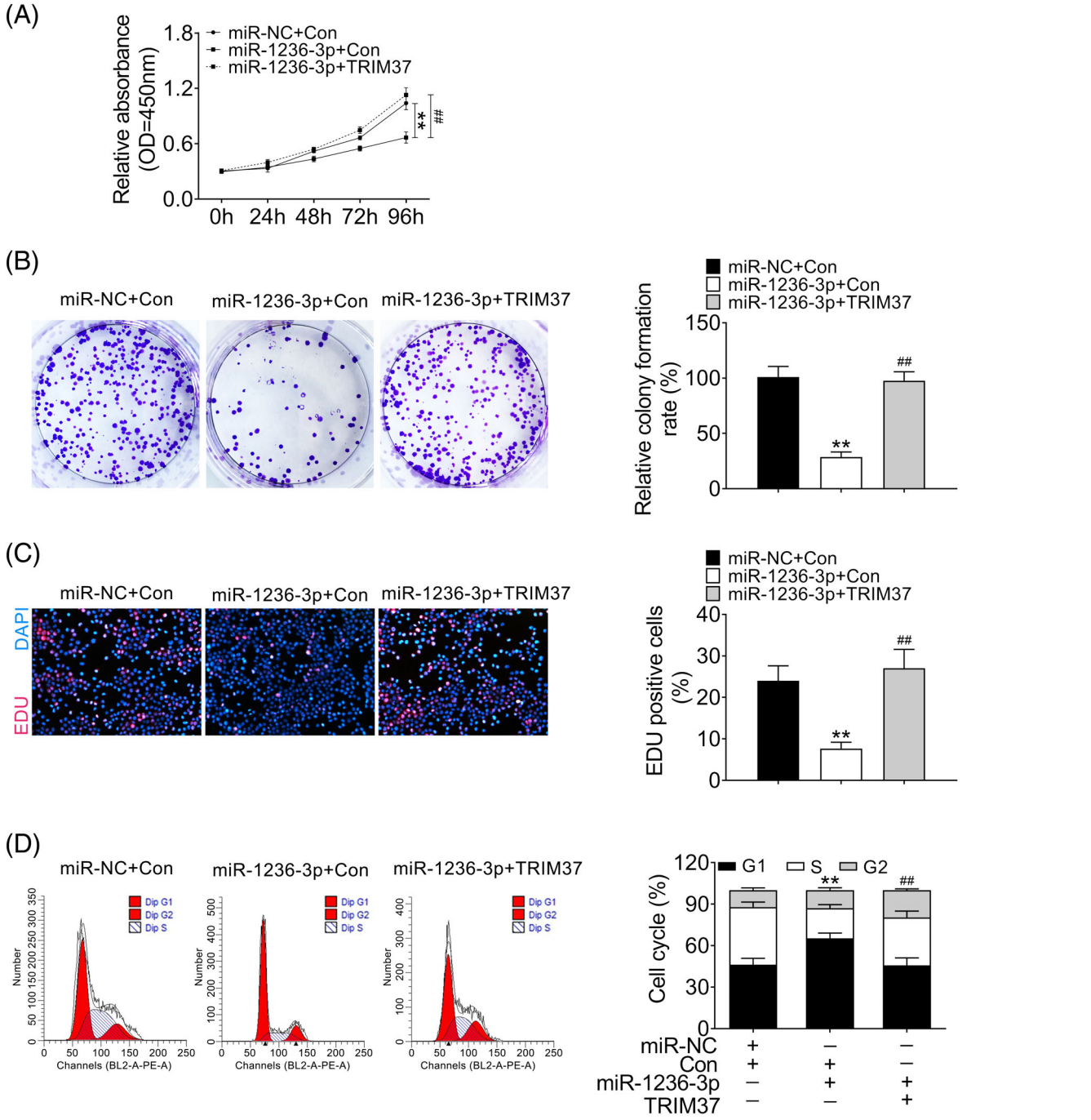

FIGURE 6 miR-1236-3p/TRIM37 affected the proliferation and cycle progression of cervical cancer cells. (A) Growth curves of SiHa or CaSki cells after transfection with miR-1236-3p + con, miR-1236-3p + TRIM37, or the corresponding control (miR-NC + con). Measurements of the cell growth rate were obtained using a CCK-8 kit. (B) Colony formation analysis of SiHa or CaSki cells expressing miR-NC + con, miR-1236-3p + con, or miR-1236-3p + TRIM37. Colony numbers were quantified. (C) Representative profiles of EDU cell growth in SiHa or CaSki cells after transfection with miR-NC + con, miR-1236-3p + con, or miR-1236-3p + TRIM37. EDU positive cell numbers were quantified. (D) Cell cycle analysis of SiHa or CaSki cells after transfection with miR-NC + con, miR-1236-3p + con, or miR-1236-3p + TRIM37. Cell percentage in G1, S, and G2 phages were quantified (mean ± SEM, */#p < 0.05, **/##p < 0.01)

4 | DISCUSSION

In this study, we not only demonstrated the regulatory functions of circRNA_101996, cell proliferation, cycle progression, and migration, but also identified a regulatory relationships between circRNA_101996 and miR-1236-3p/TRIM37. Recently, circRNAs are one of the new regulators that have been investigated in cervical cancer.[28] For example, Zhang et al. found circ_0023404 sponged oncogenic miR-136, activated TFCP2/YAP pathway and promoted cervical cancer progression.[29] Rong et al. suggested circ_0007534 exerted suppressive functions in cervical

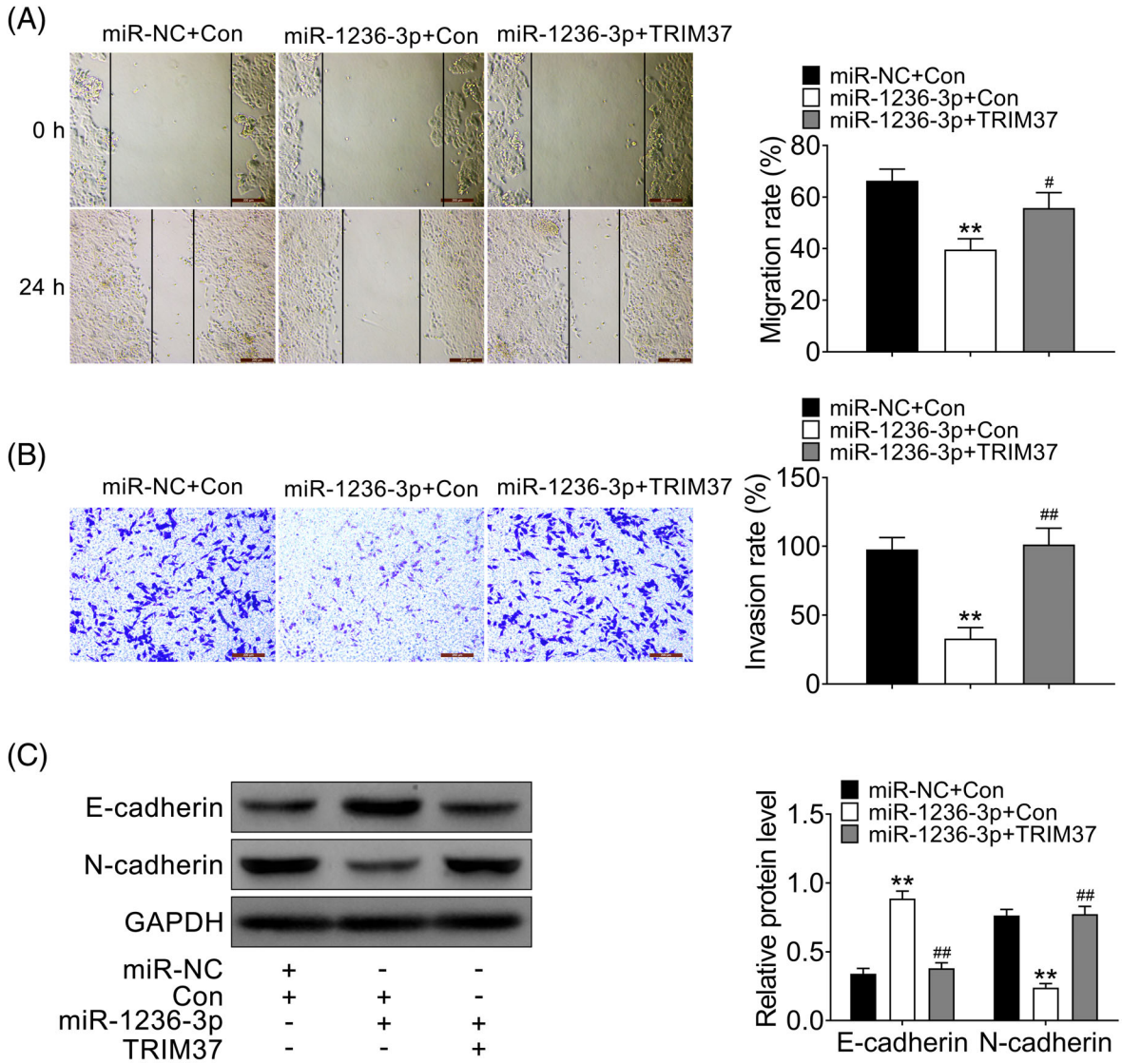

FIGURE 7 miR-1236-3p/TRIM37 affected the migration of cervical cancer cells. (A) Wound scratch healing assay of SiHa or CaSki cells after transfection with miR-NC + con, miR-1236-3p + con, or miR-1236-3p + TRIM37. Quantification of the wound-healing assay was shown as histograms. (B) Migration assay of SiHa or CaSki cells after transfection with miR-NC + con, miR-1236-3p + con, or miR-1236-3p + TRIM37. The migrated cells were quantified and shown as histograms. (C) Protein expression levels of E-cadherin and N-cadherin in SiHa or CaSki cells after transfection with miR-NC + con, miR-1236-3p + con, or miR-1236-3p + TRIM37, as determined using western blotting. Bands and images were determined by image J and shown in histogram (mean ± SEM, $^{*}p < 0.05$, $^{**}/\#\#p < 0.01$)

cancer by affecting the axis of miR-498/BMI-1.[30] Together, these studies indicated circRNAs usually exert their regulatory functions by down-regulating their target-bound miRNAs. Our previous studies found that circRNA_101996 down-regulated miR-8075, and then increased the expression of TPX2, miR-8075's target in cervical cancer cells.[11] On account of that, one circRNA might simultaneously sponge several miRNAs. Other potential miRNAs targeting circRNA_101996 and the corresponding molecular functions in cervical cancer development require further study. Our data in this study suggested that miR-1236-3p can also be targeted by circRNA_101996 in cervical cancer.

As a recently discovered miRNA, miR-1236-3p expression was first reported to be down-expressed in ovarian carcinoma.[15] In addition, it was reported that down-expression of miR-1236-3p is related to clinical tumor degree and poor prognosis of gastric cancer patients.[6] Our data demonstrated that the expression of miR-1236-3p was accordingly decreased in cervical cancer and it inhibited cell proliferation, cell cycle progression, and cell invasion through targeting TRIM37. Based on the multi-targets characteristics, other tumor related genes have also been found to be targeting by miR-1236-3p, mainly containing zinc-finger E-box binding homeobox 1 (ZEB1) in ovarian carcinoma,[13] Krueppel-like factor 8 (KLF8) in lung adenocarcinoma[14] and metastasis associated 1 family member 2 (MTA2) in gastric cancer.[31]. In contrast to these genes and TRIM44, the mRNA TRIM37 was highly expressed in cervical cancer cells (Figure S5A). Moreover, miR-1236-3p led to the strongest inhibition of the luciferase activity of the TRIM37 3′-UTR reporter plasmids (Figure S5B).

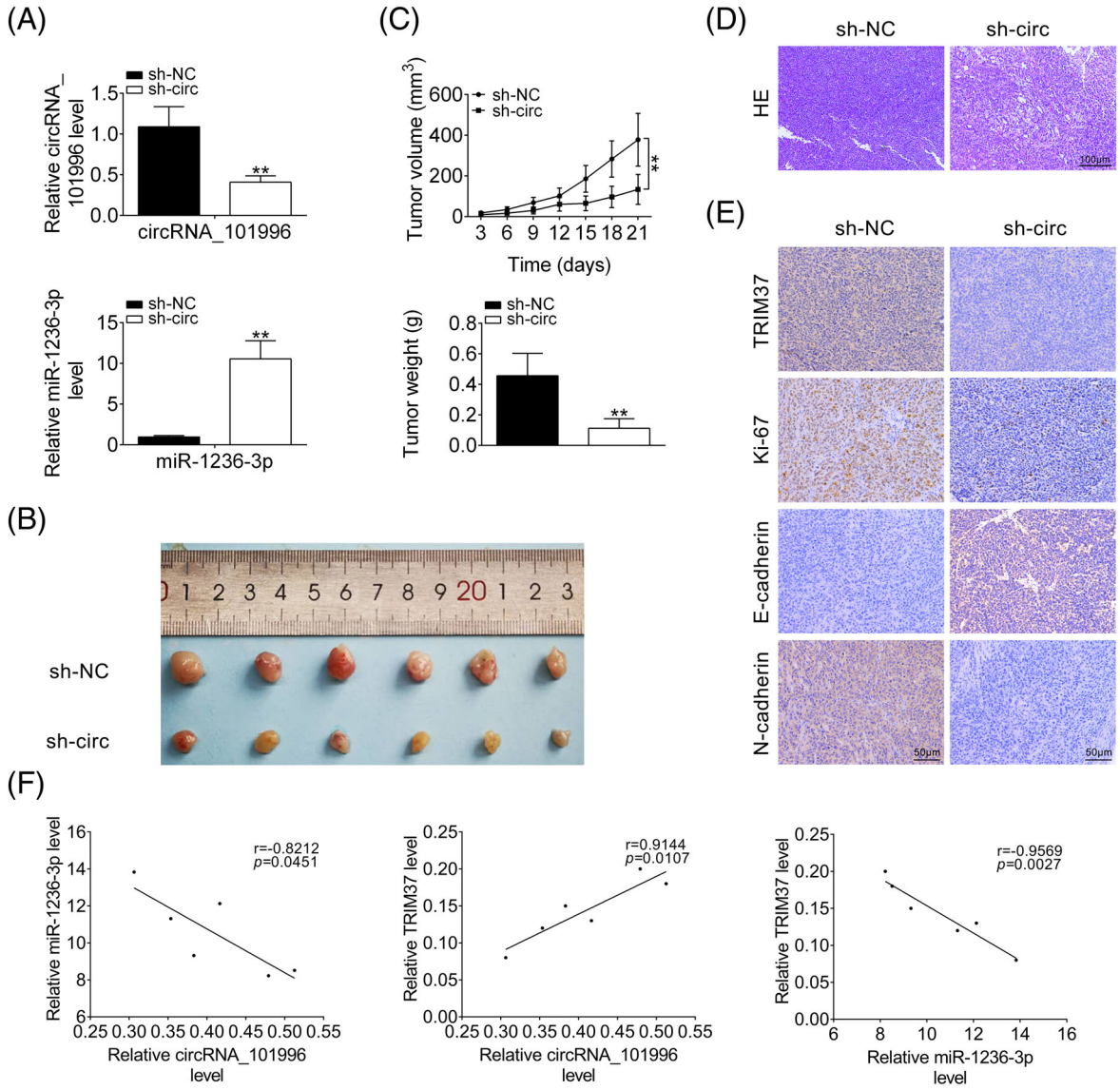

FIGURE 8 circRNA_101996 knockdown inhibited tumor growth in a cervical cancer mouse xenograft model. (A) Expression levels of circRNA_101996 and miR-1236-3p in the xenograft tumors derived from subcutaneous implantation of SiHa cells stably expressing sh-circ or sh-NC, as determined using qRT-PCR. (B) Image of corresponding tumors dissected from mice 21 days post-implantation. (C) Volumes (up) and weights (down) of the xenograft tumors derived from subcutaneous implantation of SiHa cells stably expressing sh-circ or sh-NC. (D) H&E staining and (E) IHC staining of TRIM37, Ki67, E-cadherin, and N-cadherin in the xenograft tumors derived from subcutaneous implantation of SiHa cells stably expressing sh-circ or sh-NC. Scale bar = 50 μm. (F) Pearson's correlation analysis of the relative expressions between circRNA_101996 and miR-1236-3p, miR-1236-3p and TRIM37 mRNA, circRNA_101996 and TRIM37 mRNA in in the xenograft tumors (mean ± SEM, $^{**}p < 0.01$)

Therefore, TRIM37 is demonstrated as the main target of miR-1236-3p in cervical cancer. Whether miR-1236-3p exerts its activity through negatively adjusting these genes in cervical cancer requires further investigations. The effect of circRNA_101996/miR-1236-3p on cervical cell functions might be associated with the regulation of TRIM37 and other possible targets.

TRIM37 is located on chromosome 17q23, and has an estimated molecular weight of 130 kDa.[32] It has also been found that TRIM37 may result in extensive changes in gene expression, involving in several cancers, including colon cancer, liver cancer and glioma.[23,33–34] To date, the expression pattern and the biological function of TRIM37 in cervical cancer remain to be elucidated. Our data demonstrated that the mRNA and protein expression levels of TRIM37 were up-regulated in cervical cancer, suggesting its tumor promoting effect. Previous studies have demonstrated some signaling pathways mediated by TRIM37. For example, TRIM37 was found to exert a vital role in constitutive NF-κB pathway excitation and target AKT in lung cancer.[19,35] In addition, TRIM37 knockdown suppressed the growth and metastasis of human glioma partially through the down-regulation of PI3K/Akt signaling pathway.[33] Furthermore, SIP1-mediated epithelial-mesenchymal transition and MTORC1-TFEB axis mediated autophagy were, respectively, found to be regulated by TRIM37.[21,36] However, there is no report about miRNA

mediated regulation of TRIM37 expression. Our results for the first time demonstrated that circRNA_101996 knockdown suppressed TRIM37 expression by up-regulating miR-1236-3p, which could enrich the regulation mechanism of TRIM37 and improve cervical cancer clinical treatment.

Together, our data revealed that circRNA_101996 over-expression promoted the cell proliferation, cell cycle progression and cell migration of cervical cancer cells, whereas circRNA_101996 knockdown exerted opposite effects. In addition, circRNA_101996 negatively modulated miR-1236-3p and decreased its expression. The axis of circRNA_101996/miR-1236-3p exerted an important function by regulating TRIM37 expression through targeting its 3′-UTR in cervical cancer. Moreover, the effect of circRNA_101996/miR-1236-3p/TRIM37 on cervical cancer growth was confirmed in a mouse xenograft model. On account of the effects of cell proliferation, cell cycle progression, and cell migration, the axis of circRNA_101996/miR-1236-3p/TRIM37 has the potential to be investigated as the therapeutic target for the treatment of cervical cancer.

CONFLICT OF INTEREST

All authors declare no conflict of interest.

ORCID

Xian-Chao Kong https://orcid.org/0000-0002-6594-7452

REFERENCES

1. Marth C, Landoni F, Mahner S, McCormack M, Gonzalez-Martin A, Colombo N, et al. Cervical cancer: ESMO clinical practice guidelines for diagnosis, treatment and follow-up. Ann Oncol. 2018;29:iv262.
2. Bray F, Ferlay J, Soerjomataram I, Siegel RL, Torre LA, Jemal A. Global cancer statistics 2018: GLOBOCAN estimates of incidence and mortality worldwide for 36 cancers in 185 countries. CA Cancer J Clin. 2018;68:394–424.
3. Eiben GL, da Silva DM, Fausch SC, Le Poole IC, Nishimura MI, Kast WM. Cervical cancer vaccines: recent advances in HPV research. Viral Immunol. 2003;16:111–21.
4. Speiser D, Jahn M, Ingold-Heppner B, Lanowska M, Blohmer J, Grittner U, et al. Expression of cell cycle regulators and ki67 in patients with recurrence of early cervical cancer. Eur J Gynaecol Oncol. 2018;39:76–83.
5. Improved survival with bevacizumab in advanced cervical cancer. N Engl J Med. 2017;377:702.
6. Pimple SA, Mishra GA. Global strategies for cervical cancer prevention and screening. Minerva Ginecol. 2019;71:313–20.
7. Qu S, Yang X, Li X, Wang J, Gao Y, Shang R, et al. Circular RNA: a new star of noncoding RNAs. Cancer Lett. 2015;365:141–8.
8. Huang S, Yang B, Chen BJ, Bliim N, Ueberham U, Arendt T, et al. The emerging role of circular RNAs in transcriptome regulation. Genomics. 2017;109:401–7.
9. Hansen TB, Jensen TI, Clausen BH, Bramsen JB, Finsen B, Damgaard CK, et al. Natural RNA circles function as efficient microRNA sponges. Nature. 2013;495:384–8.
10. Ambros V. The functions of animal microRNAs. Nature. 2004;431:350–5.
11. Song T, Xu A, Zhang Z, Gao F, Zhao L, Chen X, et al. CircRNA hsa_circRNA_101996 increases cervical cancer proliferation and invasion through activating TPX2 expression by restraining miR-8075. J Cell Physiol. 2019;234:14296–305.
12. An JX, Ma ZS, Ma MH, Shao S, Cao FL, Dai DQ. MiR-1236-3p serves as a new diagnostic and prognostic biomarker for gastric cancer. Cancer Biomark. 2019;25:127–32.
13. Zhu XP, Wang XL, Ma J, Fang YF, Zhang HJ, Zhang C, et al. Down-regulation of miR-1236-3p is correlated with clinical progression and unfavorable prognosis in gastric cancer. Eur Rev Med Pharmacol Sci. 2018;22:5914–19.
14. Bian T, Jiang D, Liu J, Yuan X, Feng J, Li Q, et al. miR-1236-3p suppresses the migration and invasion by targeting KLF8 in lung adenocarcinoma A549 cells. Biochem Biophys Res Commun. 2017;492:461–7.
15. Wang Y, Yan S, Liu X, Zhang W, Li Y, Dong R, et al. miR-1236-3p represses the cell migration and invasion abilities by targeting ZEB1 in high-grade serous ovarian carcinoma. Oncol Rep. 2014;31:1905–10.
16. Hatakeyama S. TRIM proteins and cancer. Nat Rev Cancer. 2011;11:792–804.
17. Nisole S, Stoye JP, Saib A. TRIM family proteins: retroviral restriction and antiviral defence. Nat Rev Microbiol. 2005;3:799–808.
18. Bhatnagar S, Gazin C, Chamberlain L, Ou J, Zhu X, Tushir JS, et al. TRIM37 is a new histone H2A ubiquitin ligase and breast cancer oncoprotein. Nature. 2014;516:116–20.
19. Li Y, Deng L, Zhao X, Li B, Ren D, Yu L, et al. Tripartite motif-containing 37 (TRIM37) promotes the aggressiveness of non-small-cell lung cancer cells by activating the NF-kappaB pathway. J Pathol. 2018;246:366–78.
20. Kabekkodu SP, Shukla V, Varghese VK, Adiga D, Vethil Jishnu P, Chakrabarty S, et al. Cluster miRNAs and cancer: diagnostic, prognostic and therapeutic opportunities. Wiley Interdiscip Rev RNA. 2019;11(2):e1563.
21. Chen D, You X, Pan Y, Liu Q, Cao G. TRIM37 promotes cell invasion and metastasis by regulating SIP1-mediated epithelial-mesenchymal transition in gastric cancer. Onco Targets Ther. 2018;11:8803–13.
22. Zhao P, Guan HT, Dai ZJ, Ma YG, Liu XX, Wang XJ. Knockdown of tripartite motif-containing protein 37 (TRIM37) inhibits the proliferation and tumorigenesis in colorectal cancer cells. Oncol Res. 2017;25:115–22.
23. Jiang J, Yu C, Chen M, Tian S, Sun C. Over-expression of TRIM37 promotes cell migration and metastasis in hepatocellular carcinoma by activating Wnt/beta-catenin signaling. Biochem Biophys Res Commun. 2015;464:1120–27.
24. de Planell-Saguer M, Rodicio MC, Mourelatos Z. Rapid in situ codetection of noncoding RNAs and proteins in cells and formalin-fixed paraffin-embedded tissue sections without protease treatment. Nat Protoc. 2010;5:1061–73.
25. Hu Y, Liu Q, Zhang M, Yan Y, Yu H, Ge L. MicroRNA-362-3p attenuates motor deficit following spinal cord injury via targeting paired box gene 2. J Integr Neurosci. 2019;18:57–64.
26. Ma G, Tang M, Wu Y, Xu X, Pan F, Xu R. LncRNAs and miRNAs: potential biomarkers and therapeutic targets for prostate cancer. Am J Transl Res. 2016;8:5141–50.
27. Kastenmayer RJ, Moore RM, Bright AL, Torres-Cruz R, Elkins WR. Select agent and toxin regulations: beyond the eighth edition of the guide for the care and use of laboratory animals. J Am Assoc Lab Anim Sci. 2012;51:333–8.
28. Chaichian S, Shafabakhsh R, Mirhashemi SM, Moazzami B, Asemi Z. Circular RNAs: a novel biomarker for cervical cancer. J Cell Physiol. 2019;235(2):718–24.
29. Zhang J, Zhao X, Zhang J, Zheng X, Li F. Circular RNA hsa_circ_0023404 exerts an oncogenic role in cervical cancer through regulating miR-136/TFCP2/YAP pathway. Biochem Biophys Res Commun. 2018;501:428–33.
30. Rong X, Gao W, Yang X, Guo J. Downregulation of hsa_circ_0007534 restricts the proliferation and invasion of cervical cancer through regulating miR-498/BMI-1 signaling. Life Sci. 2019;235:116785.
31. An JX, Ma MH, Zhang CD, Shao S, Zhou NM, Dai DQ. miR-1236-3p inhibits invasion and metastasis in gastric cancer by targeting MTA2. Cancer Cell Int. 2018;18:66.
32. Kallijarvi J, Avela K, Lipsanen-Nyman M, Ulmanen I, Lehesjoki AE. The TRIM37 gene encodes a peroxisomal RING-B-box-coiled-coil

protein: classification of mulibrey nanism as a new peroxisomal disorder. Am J Hum Genet. 2002;70:1215–28.
33. Tang SL, Gao YL, Wen-Zhong H. Knockdown of TRIM37 suppresses the proliferation, migration and invasion of glioma cells through the inactivation of PI3K/Akt signaling pathway. Biomed Pharmacother. 2018;99:59–64.
34. Hu CE, Gan J. TRIM37 promotes epithelialmesenchymal transition in colorectal cancer. Mol Med Rep. 2017;15:1057–62.
35. Dong S, Pang X, Sun H, Yuan C, Mu C, Zheng S. TRIM37 targets AKT in the growth of lung cancer cells. Onco Targets Ther. 2018;11:7935–45.
36. Wang W, Xia Z, Farre JC, Subramani S. TRIM37 deficiency induces autophagy through deregulating the MTORC1-TFEB axis. Autophagy. 2018;14:1574–85.

SUPPORTING INFORMATION

Additional supporting information may be found online in the Supporting Information section at the end of this article.

How to cite this article: Song T-F, Xu A-L, Chen X-H, Gao J-Y, Gao F, Kong X-C. Circular RNA circRNA_101996 promoted cervical cancer development by regulating miR-1236-3p/TRIM37 axis. *Kaohsiung J Med Sci*. 2021;37:547–561. https://doi.org/10.1002/kjm2.12378